Electronics and Communications in Japan, Part 2, Vol. 82, No. 12, 1999
Translated from Denshi Joho Tsushin Gakkai Ronbunshi, Vol. J82-C-I, No. 4, April 1999, pp. 175–183

Analysis of Infinitely Thin Dielectric Gratings with Surface Relief

Hideaki Wakabayashi and Jiro Yamakita

Faculty of Computer Science and System Engineering, Okayama Prefectural University, Soja, Japan 719-1197

Keiji Matsumoto

Faculty of Engineering, Osaka Sangyo University, Daito, Japan 574-8530

Masamitsu Asai

Faculty of Biology-Oriented Science and Technology, Kinki University, Wakayama, Japan 649-6493

SUMMARY

The spectral Galerkin procedure is often used for analyzing metallic gratings which are assumed to be zero-thickness plane gratings. In this report, thin surface relief dielectric gratings with complex permittivity are discussed and analyzed by using the numerical approach for metallic plane gratings with surface impedance. From numerical results for dielectric gratings by the conventional method and metallic plane gratings by the spectral Galerkin procedure, the relations between dielectric and plane gratings are investigated. In addition, some numerical results for infinitely thin gratings with various surface reliefs are given and the differences between surface profiles are investigated. © 1999 Scripta Technica, Electron Comm Jpn Pt 2, 82(12): 38–47, 1999

Key words: Plane metallic grating; resistive boundary condition; spectral Galerkin procedure; surface relief dielectric grating.

1. Introduction

Analysis of electromagnetic scattering by plane metallic gratings is one of the fundamental problems in electromagnetic field theory. Many authors have reported analyses of resistive gratings in addition to perfectly conducting gratings [1–4].

In the analysis of a resistive plane grating, by assuming that grating layer defined by complex permittivity and thickness has zero thickness, a rectangular dielectric grating is replaced by surface resistance. The calculations are carried out so that the surface resistance and the current distribution satisfy the boundary condition. In other words, a dielectric grating in which the imaginary part of the permittivity is very large and in which the thickness is thin compared with skin depth is considered a resistive plane grating. The current expansion and the resistive boundary condition, based on the assumption that the current density is traveling on the surface, are introduced.

The spectral Galerkin procedure [5, 6] is a popular method for the scattering problem of plane gratings, since the numerically acceptable solutions can be obtained in a

CCC8756-663X/99/120038-10

small number of current expansions by application to the resistive boundary condition. In addition, this procedure involves less voluminous and simpler computation than the procedure for dielectric gratings.

We have investigated the limits of thickness in the applicability of the current expansion and the resistive boundary condition for one-dimensional gratings. By comparing the numerical results between thin rectangular dielectric gratings and resistive–reactive plane gratings [7, 8], we reported that very thin dielectric gratings can be analyzed by using the numerical approach for plane gratings [9, 10].

In this paper, we demonstrate that surface relief dielectric gratings with various profiles can be treated as a plane grating with surface impedance as a function of the position parameter. For clarity, we consider one-dimensional gratings and examine the cases of resistive and reactive gratings separately [11, 12]. Additionally, some numerical results for infinitely thin dielectric gratings are given and the differences between surface profiles are discussed.

2. Setting of the Problem

As shown in Fig. 1, a one-dimensional grating with periodicity Λ and width W placed on a dielectric substrate is uniform along the y-direction. Panels (a) and (b) show a very thin surface relief dielectric grating with various profiles $x(z)$ and a plane grating with surface impedance $R(z)$ as a function of the position parameter z, respectively. Let us consider scattering from the gratings by a plane wave $\exp[j\{\omega t - \sqrt{\varepsilon_1}k_0(x\cos\theta_i + z\sin\theta_i)\}]$ at an incidence angle

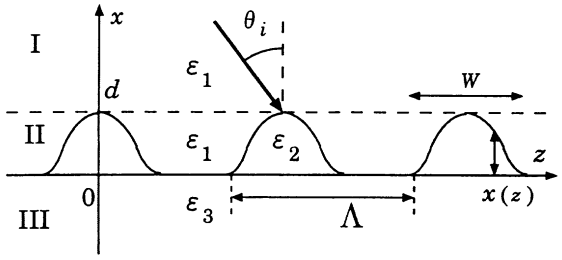

(a) Thin dielectric grating

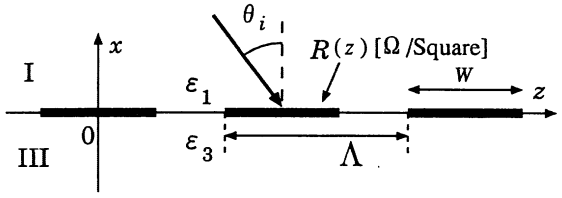

(b) Plane grating

Fig. 1. Dielectric and plane gratings.

θ_i. The regions I and III with relative permittivity ε_1 and ε_3 are lossless materials, and the imaginary part of the relative permittivity is ignored. In panel (a), the grating layer in region II is described by relative permittivity $\varepsilon_2 = \varepsilon_2' - i\varepsilon_2''$ and thickness $x(z) = df(z)$, where d is the groove depth of the grating. Since the grating in the region $x \geq 0$ is surrounded by air, we assume that the real part of the relative permittivity is $\varepsilon_2' = \varepsilon_1 = 1$ throughout this paper. If the thickness tends to zero and the conductivity varies in such a way that the product σd keeps a finite value, the dielectric grating can be approximated to a resistive–reactive plane grating in panel (b) by using

$$R(z) = \frac{1}{\sigma x(z)} = \frac{1}{(1/Z_0)k_0\, x(z)\, \varepsilon_2''} = \frac{1}{f(z)}\, R_0 \qquad (1)$$

where R_0 is the impedance value in the maximum thickness on the surface profile. $R(z)$ is described by the surface impedance, with the components of resistance and reactance [10, 13].

In the following theory, we normalize the space variables (x, y, z) by the wave number in vacuum $k_0 = \omega\sqrt{\varepsilon\mu} = 2\pi/\lambda$ such that $k_0 x \to x$, $k_0 y \to y$, and $k_0 z \to z$.

Since the structure is periodic, electromagnetic fields E_l and H_l $(l = x, y, z)$ are expressed in terms of spatial harmonics with expansion coefficients e_{lm} and h_{lm}:

$$\sqrt{Y_0}E_\ell = \sum_{m=-M}^{M} e_{\ell m}(x)\exp(-is_m z) \qquad (2)$$

$$\sqrt{Z_0}H_\ell = \sum_{m=-M}^{M} h_{\ell m}(x)\exp(-is_m z) \qquad (3)$$

$$s_m = s_0 + m\lambda/\Lambda, \qquad s_0 = \sqrt{\varepsilon_1}\sin\theta_i \qquad (4)$$

Using the normalized space variables, the Maxwell equations take dimensionless form (which is analytically simple in computational electromagnetics) and can be rewritten as

$$\overline{\text{curl}}\,\sqrt{Y_0}\boldsymbol{E} = -i\sqrt{Z_0}\boldsymbol{H} \qquad (5)$$

$$\overline{\text{curl}}\,\sqrt{Z_0}\boldsymbol{H} = i\,\varepsilon(z)\sqrt{Y_0}\boldsymbol{E} \qquad (6)$$

where $Z_0 = 1/Y_0 = \sqrt{\mu_0/\varepsilon_0}$ and $\overline{\text{curl}}$ is the curl for the normalized space variables.

3. Method of Analysis for a Dielectric Grating

The conventional method of solving the eigenvalue problem of the coupling matrix is applied to a dielectric grating in Fig. 1(a) [14].

Since the structure is periodic, the relative permittivity $\varepsilon_2(x, z)$ in the grating layer is expanded as a Fourier series of N_f terms with Fourier coefficients $b_m(x)$:

$$\varepsilon_2(x,z) = \sum_{m=-N_f}^{N_f} b_m(x) \exp\{im(\lambda/\Lambda)z\} \tag{7}$$

The quantities $\boldsymbol{e}_l(x)$ and $\boldsymbol{h}_l(x)$ are the $(2M+1)$-dimensional row vectors of the expansion coefficients for the tangential field components:

$$\boldsymbol{e}_\ell(x) = [e_{\ell-M}(x) \dots e_{\ell 0}(x) \dots e_{\ell M}(x)]^t \tag{8}$$

$$\boldsymbol{h}_\ell(x) = [h_{\ell-M}(x) \dots h_{\ell 0}(x) \dots h_{\ell M}(x)]^t \tag{9}$$

The differential equations for the y and z field components can be derived as follows:

$$\frac{d\boldsymbol{F}}{dx} = i\, \boldsymbol{C}\, \boldsymbol{F}(x) \tag{10}$$

TE waves:

$$\boldsymbol{F} = \begin{bmatrix} \boldsymbol{e}_y \\ \boldsymbol{h}_z \end{bmatrix}, \quad \boldsymbol{C} = \begin{bmatrix} [0] & -[1] \\ -[\varepsilon] + [s]^2 & [0] \end{bmatrix} \tag{11}$$

TM waves:

$$\boldsymbol{F} = \begin{bmatrix} \boldsymbol{e}_z \\ \boldsymbol{h}_y \end{bmatrix}, \quad \boldsymbol{C} = \begin{bmatrix} [0] & [1] - [s][\varepsilon]^{-1}[s] \\ [\varepsilon] & [0] \end{bmatrix} \tag{12}$$

where $[C]$ consists of $m \times n$ submatrices:

$$[\varepsilon] = [b_{n-m}],\ [s] = [s_m \delta_{mn}],\ [1] = [\delta_{mn}] \tag{13}$$

$[0]$ is a zero matrix, $[\varepsilon]^{-1}$ is the inverse matrix of $[\varepsilon]$, and δ_{mn} is the Kronecker delta. By using the $2(2M+1)$-dimensional row vector $\boldsymbol{a}(x)$ and transforming

$$\boldsymbol{F}(x) = \boldsymbol{T}\, \boldsymbol{a}(x) \tag{14}$$

the solution of Eq. (10) is given by

$$\boldsymbol{F}(x) = \boldsymbol{T}\, [\exp\{i\, \kappa_m (x - x_0)\} \delta_{mn}]\, \boldsymbol{a}(x_0) \tag{15}$$

where κ is an eigenvalue and $[T]$ is a diagonalization matrix. The eigenvalues in regions I and III can be obtained analytically:

$$\kappa_m^{\pm} = \mp \xi_m = \mp \sqrt{\varepsilon - s_m^2} \tag{16}$$

$\boldsymbol{a}(x)$ can be decomposed into complex amplitudes $\boldsymbol{a}^{\pm}$ corresponding to the propagating directions determined by the sign of κ. When ξ_m has a complex value, the sign is chosen such that the imaginary part becomes a negative quantity. The eigenvectors are normalized to $e_{ym} h_{zm}^* = \pm\, \xi_m$ and $-e_{zm} h_{ym}^* = \pm\, \xi_m$. The grating layer is approximated by partitioning into stratified multilayers with $(L-2)$ rectangular gratings, as represented in Fig. 2. From the boundary conditions at each interface, we have

$$x = x_1 = d:$$

$$[T_1] \begin{bmatrix} \boldsymbol{a}_1^+(x_1) \\ \boldsymbol{a}_1^-(x_1) \end{bmatrix} = [T_2] \begin{bmatrix} [U(\kappa_2^+, x_1 - x_2)] & [0] \\ [0] & [1] \end{bmatrix} \begin{bmatrix} \boldsymbol{a}_2^+(x_2) \\ \boldsymbol{a}_2^-(x_1) \end{bmatrix} \tag{17}$$

$$x = x_n \quad (n = 2 \cdots L-2):$$

$$[T_n] \begin{bmatrix} [1] & [0] \\ [0] & [U(\kappa_n^-, x_{n-1} - x_n)] \end{bmatrix} \begin{bmatrix} \boldsymbol{a}_n^+(x_n) \\ \boldsymbol{a}_n^-(x_{n-1}) \end{bmatrix} = [T_{n+1}] \begin{bmatrix} [U(\kappa_{n+1}^+, x_n - x_{n+1})] & [0] \\ [0] & [1] \end{bmatrix} \cdot \begin{bmatrix} \boldsymbol{a}_{n+1}^+(x_{n+1}) \\ \boldsymbol{a}_{n+1}^-(x_n) \end{bmatrix} \tag{18}$$

$$x = x_{L-1} = 0:$$

$$[T_{L-1}] \begin{bmatrix} [1] & [0] \\ [0] & [U(\kappa_{L-1}^-, x_{L-2} - x_{L-1})] \end{bmatrix} \cdot \begin{bmatrix} \boldsymbol{a}_{L-1}^+(x_{L-1}) \\ \boldsymbol{a}_{L-1}^-(x_{L-2}) \end{bmatrix} = [T_L] \begin{bmatrix} \boldsymbol{a}_L^+(x_{L-1}) \\ \boldsymbol{a}_L^-(x_{L-1}) \end{bmatrix} \tag{19}$$

$$\boldsymbol{a}_1^- = [0 \cdots 1 \cdots 0]^t, \quad \boldsymbol{a}_L^+ = [0 \cdots 0 \cdots 0]^t \tag{20}$$

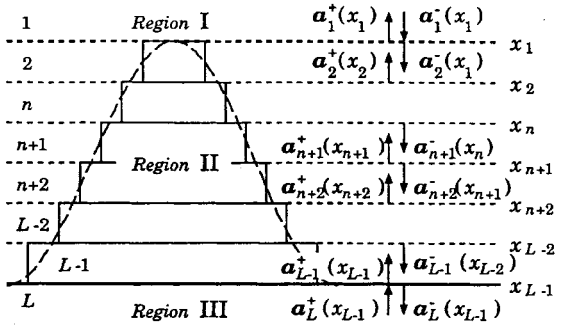

Fig. 2. Partitioning of grating region into multilayers with rectangular gratings.

The unknowns are $\boldsymbol{a}_1^+(x_1)$ and $\boldsymbol{a}_L^-(x_{L-1})$. The m-th mode diffraction efficiency η_m^r of the reflected wave and that η_m^t of the transmitted wave are given by

$$\eta_m^r = \frac{|\,Re\{\kappa_{1m}^+\}\,|\,|\,a_{1m}^+(x_1)\,|^2}{|\,Re\{\kappa_{10}^-\}\,|} \tag{21}$$

$$\eta_m^t = \frac{|\,Re\{\kappa_{Lm}^-\}\,|\,|\,a_{Lm}^-(x_{L-1})\,|^2}{|\,Re\{\kappa_{10}^-\}\,|} \tag{22}$$

4. Method of Analysis for a Plane Grating

Applying the spectral Galerkin procedure to a plane grating, and assuming that the parameter of thickness can be ignored, solutions can be obtained with a small number of the current expansion terms.

A resistive boundary condition can be characterized by using the tangential electric field $E_{\tan}(x, z)$ at the interface $x = 0$, the surface resistance $R(z)$ as a function of position parameter z, and the current density $J(x, z)$ as follows:

$$\sqrt{Y_0}E_{\tan}(z) - (R(z)/Z_0)\sqrt{Z_0}J(z) = 0 \qquad (-W/2 \leqq z \leqq W/2) \tag{23}$$

The tangential electric field and the current density refer to $E_{\tan} = E_y$ and $J = J_y$ in the TE case or E_z and J_z in the TM case, respectively. It is easy to distinguish between the two cases in the analysis of a one-dimensional grating and the subscripts are omitted in the following formulas.

The total fields are given by the sum of the primary field $E_{\tan}^{1st}(z)$ with the grating strips removed and the scattered field $E_{\tan}^{2nd}(z)$ radiated by the source of electric current $J(z)$ as follows:

$$\begin{aligned}&\sqrt{Y_0}E_{\tan}(z)\\ &= \sqrt{Y_0}\{E_{\tan}^{1st}(z) + E_{\tan}^{2nd}(z)\}\\ &= \overline{e_0(0)}\exp(-is_0z)\\ &\quad + \sum_{m=-M}^{M} g_m(0)j_m\exp(-is_mz)\end{aligned} \tag{24}$$

where $g_m(x)$ is a Green's function in the spectral domain and j_m is the expansion coefficient of surface current, expressed in terms of the spatial harmonics:

$$\sqrt{Z_0}J(z) = \sum_{m=-M}^{M} j_m\exp(-is_mz) \tag{25}$$

Let the surface current $J(z)$ be expanded in a set of N basis functions $\Phi_p(z)$, as

$$\sqrt{Z_0}J(z) = \sum_{p=1}^{N} I_p\ \Phi_p(z) \tag{26}$$

Application of the spectral Galerkin procedure yields

$$[A_{kp}]\ [I_p] = [b_k] \qquad (k = 1, 2, \cdots, N) \tag{27}$$

$$A_{kp} = \sum_{p=1}^{N}\left[\sum_{m=-M}^{M}\phi_{mk}^*\ g_m(0)\ \phi_{mp} - \frac{1}{\Lambda}\int_{-W/2}^{W/2}\Phi_k^*\ (R(z)/Z_0)\ \Phi_p\ dz\right] \tag{28}$$

$$\begin{aligned}b_k &= -\frac{\overline{e_0(0)}}{\Lambda}\int_{-W/2}^{W/2}\Phi_k^*(z)\exp(-is_0z)dz\\ &= -\overline{e_0(0)}\ \phi_{0k}^*\end{aligned} \tag{29}$$

which is a set of N linear equations for the unknown coefficient I_p. Once I_p is found, the current distribution $J(z)$ can be determined. By using the method of solving the eigenvalue problem in Section 3, the Green's function $g_m(x)$ can be easily introduced. Taking the truncation number of the Fourier series to be $2N_f + 1 = 1$, the analytic model is equivalent to a nonperiodic multilayer. Accordingly, the Green's function for a source of the electric current j_m is analytically obtained for the normalized propagation constant s_m [10, 15]. The reflected and transmitted diffraction efficiencies of the m-th mode are given by

$$\eta_m^r = \frac{|\,Re\{\kappa_{1m}^+\}\,|\,|\,g_{1m}^+(0)\ j_m + g_{10}^+(0)\ \delta_{0m}\,|^2}{|\,Re\{\kappa_{10}^-\}\,|} \tag{30}$$

$$\eta_m^t = \frac{|\,Re\{\kappa_{3m}^-\}\,|\,|\,g_{3m}^-(0)\ j_m + g_{30}^-(0)\ \delta_{0m}\,|^2}{|\,Re\{\kappa_{10}^-\}\,|} \tag{31}$$

5. Numerical Results

In this paper we show some numerical results for one-dimensional gratings with rectangular, sinusoidal, triangular, and asymmetric triangular profiles stated by a function $f(z)$ and propose that very thin dielectric gratings with surface relief can be analyzed by the numerical approach for plane gratings. For simplicity, we verify the cases of resistive and reactive gratings separately:

$$f(z) = \begin{cases}\dfrac{1}{2} & \text{(rectangular)}\\ \dfrac{1}{2}\{1 + \cos(2\pi\dfrac{z}{W})\} & \text{(sinusoidal)}\\ 1 - \dfrac{2}{W}|z| & \text{(triangular)}\\ \dfrac{1}{W}z + \dfrac{1}{2} & \text{(asymmetric triangular)}\end{cases} \qquad (-W/2 \leq z \leq W/2) \tag{32}$$

To allow comparison of properties between various gratings, $f(z)$ has been chosen subject to the relation that $\int_{-W/2}^{W/2} x(z)\,dz$ remains constant with changing grating thickness $x(z)$. In the case of a rectangular grating, the groove depth is $d/2(= d')$ and the resistive impedance is $2R_0$ Ω/square in practice. It is difficult and not useful to analyze a grating which has very large periodicity by using the spatial harmonic expansion method discussed in Section 3. Thus, we calculate for $\Lambda/\lambda = 0.2 \sim 2$.

In the following numerical results, regions I and III refer to the air and a lossless dielectric grating with relative permittivity $\varepsilon_3 = 2.5$, respectively. In the analyses of dielectric gratings, the numbers of the spatial harmonic expansion terms and the multilayers in region II are determined by the convergence of solutions and the computational time. In the analyses of plane gratings, the spatial harmonic expansion terms of the surface current are truncated to $2M + 1 = 301$. In order to approximate the current distributions, we use the step function as the basis function and take $N = 100$ as the expansion number. With these truncation numbers for plane gratings, the convergence of the solutions is fairly good.

First, we consider scattering by one-dimensional gratings with periodicity $\Lambda/\lambda = 0.5$ and width $W/\Lambda = 0.5$. We compare the current distributions on rectangular dielectric gratings which have groove depths $d'/\lambda = 0.1$, 0.01, 0.001 and on plane gratings. A resistive grating corresponds to electric loss, while a reactive grating corresponds to inductance in the TE case or capacitance in the TM case [16]. The cases of resistive gratings with $R_0 = 10$ Ω/square are shown in Fig. 3. The cases of reactive gratings with $R_0 = i\ 10$ Ω/square (TE wave) and with $R_0 = -i\ 10$ Ω/square (TM wave) are shown in Fig. 4. A jump of the tangential magnetic fields between the surface of the dielectric grating and the interface x_{L-1} in region III is considered to be an electric current $\sqrt{Z_0}J(z)$ and is compared with the current distribution on the plane grating. We note that the surface of the grating is assigned to the surface of the partitioned

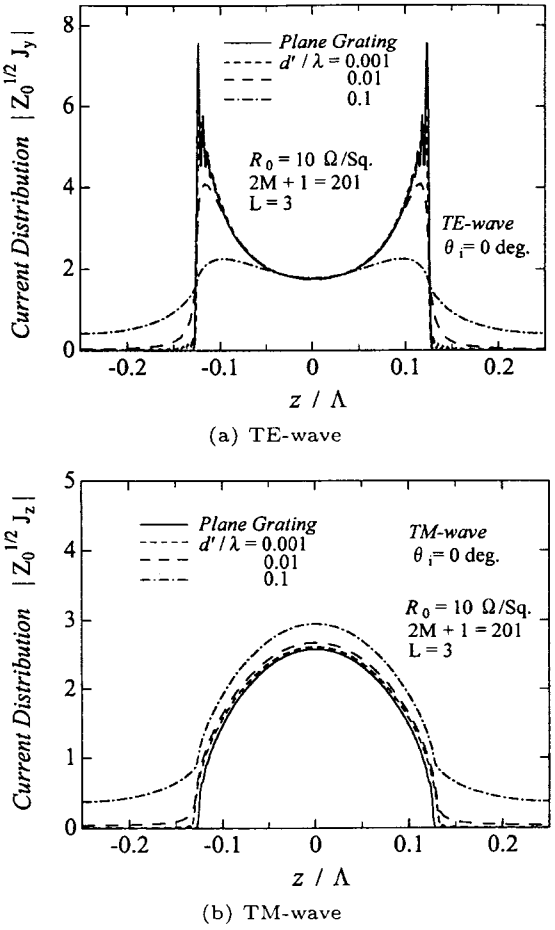

Fig. 3. Current distributions on resistive gratings with rectangular profile.

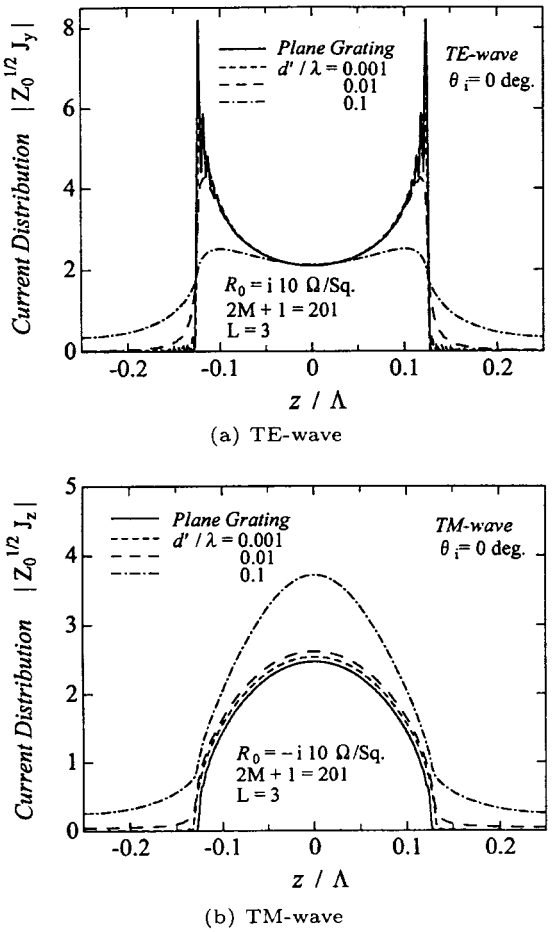

Fig. 4. Current distributions on reactive gratings with rectangular profile.

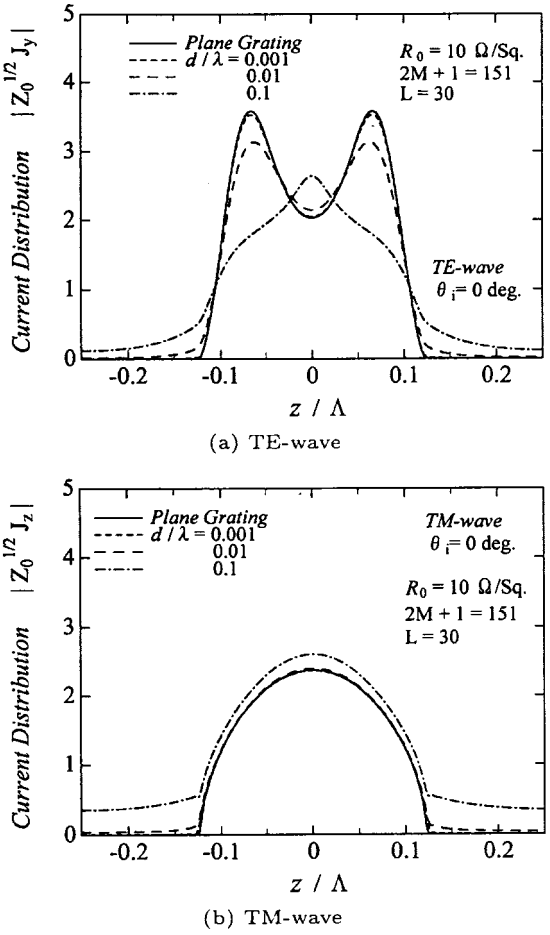

Fig. 5. Current distributions on resistive gratings with sinusoidal profile.

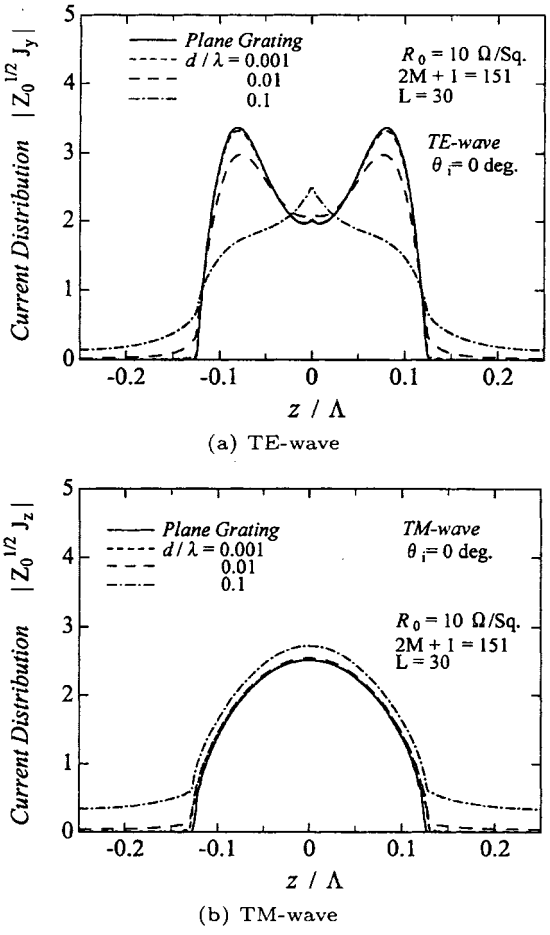

Fig. 6. Current distributions on resistive gratings with triangular profile.

multilayers in the stratified approximated model (see Fig. 2). When the groove depth is $d'/\lambda = 0.001$, the results for the dielectric gratings are in close agreement with those for the plane gratings in the TE and TM cases. The current distributions on the resistive and reactive gratings have similar tendencies. In the TE case, the effects of edge singularity appear in the results for dielectric gratings with groove depth $d'/\lambda = 0.01$, 0.001 and for plane gratings.

Figures 5 and 6 show the cases of sinusoidal and triangular resistive gratings, respectively. The results for dielectric gratings agree well with those for plane gratings when the groove depth is $d/\lambda = 0.001$. In the case of TE incidence, the effects of the edge singularity look small. Since in the case of TM incidence presented in Figs. 3(b), 4(b), 5(b), and 6(b), the electric field components are perpendicular to the gratings, the difference in the current distributions between various profiles is small. By comparison of the current distributions in Figs. 3 to 6, we have shown that when the groove depth is $d/\lambda \leq 10^{-3}$, a dielectric grating with surface relief can be treated as a plane grating.

For sinusoidal dielectric gratings with groove depth $d/\lambda = 0.1$, 0.05, 0.01 and plane gratings (periodicity $\Lambda/\lambda = 0.5$, width $W/\Lambda = 0.5$), the Joule loss versus surface resistance and relative power versus surface reactance are plotted in Figs. 7 and 8, respectively. The Joule loss is defined as $(1 - r_p - t_p)$ using the power reflected coefficient r_p $(= \sum_{m=-M}^{M} \eta_m^r)$ and the power transmitted coefficient t_p $(= \sum_{m=-M}^{M} \eta_m^t)$. In the case of the current distributions, the results for a dielectric grating with groove depth $d/\lambda = 10^{-3}$ and those for a plane grating are in close agreement. However, in the case of the scattering properties, the results for a dielectric grating with groove depth $d/\lambda = 10^{-2}$ and those for a plane grating are in close agreement, as shown in Figs. 7 and 8 [11].

Next, as an example of asymmetric profile we consider an asymmetric triangular surface profile. The ampli-

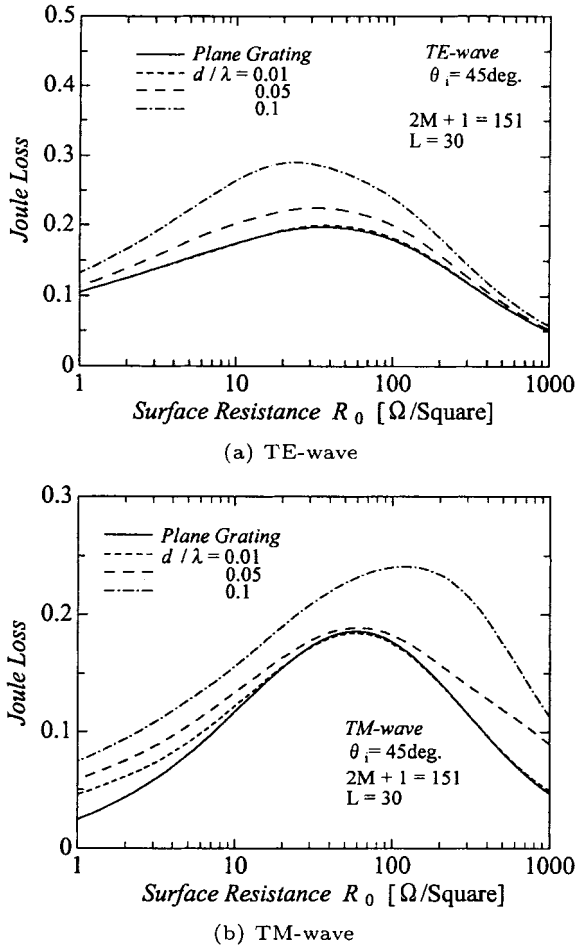

Fig. 7. Joule losses of resistive gratings with sinusoidal profile.

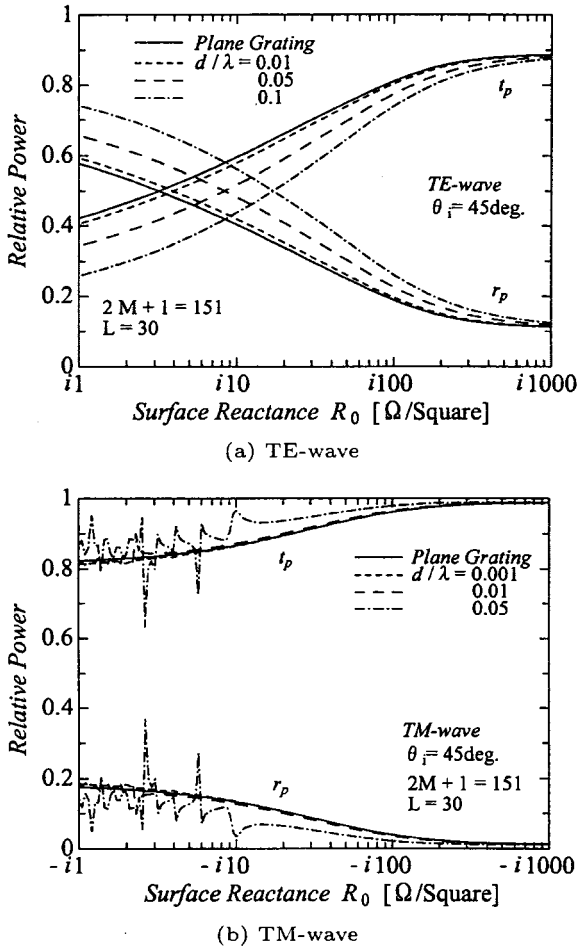

Fig. 8. Relative power of reactive gratings with sinusoidal profile.

tude reflected coefficients $r_0 = \sqrt{\eta_0^r}$ (0-th order diffracted wave) of a dielectric grating with groove depth $d/\lambda = 10^{-2}$ and a plane grating are examined in Fig. 9. In the TE and TM cases, both results are in close agreement over a wide range of grating widths W/Λ and periodicities Λ/λ. Accordingly, an infinitely thin dielectric grating can be analyzed by the numerical approach for a plane grating.

In addition, the results for infinitely thin rectangular, sinusoidal, and triangular resistive gratings (periodicity $\Lambda/\lambda = 0.5$, width $W/\lambda = 0.5$) as illustrated in Fig. 10 are discussed numerically by making use of the numerical approach for plane gratings. The current distributions on resistive gratings with surface resistance $R_0 = 100$ Ω/square are plotted together in Fig. 11. In the TE case of Fig. 11(a), the current distributions differ from those of $R_0 = 10$ Ω/square. For $R_0 = 100$ Ω/square, the effects of edge singularity appear in the results for the rectangular grating and look small in the results for the sinusoidal and triangular gratings. In the TM case of Fig. 11(b), there is small difference in the current distributions between various profiles, as demonstrated in the case of $R_0 = 10$ Ω/square.

Figures 12 and 13 show the Joule loss versus surface resistance in resistive gratings and the relative power versus surface reactance in reactive gratings, respectively. From Fig. 12, it is found that the Joule loss peaks at the same value of the surface resistance. Since gratings with very small and large resistance are equivalent to perfectly conducting and lossless dielectric materials, respectively, the Joule loss approaches 0. From Figs. 12 and 13, the difference in scattering properties between various profiles is significant in the TE case but not in the TM case. This is the same behavior as the current distributions (see Fig. 11). As a result of our investigations, we have found that the difference between surface profiles is large in the TE case.

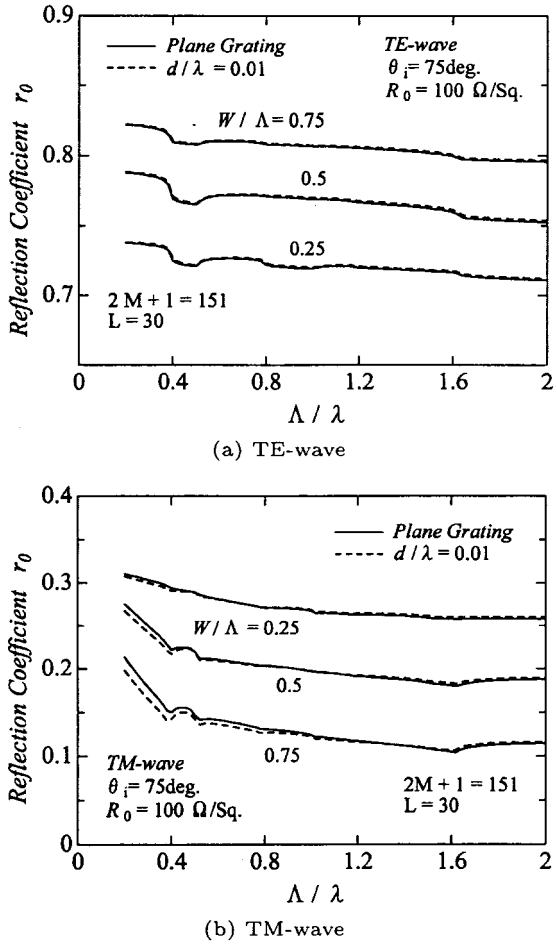

Fig. 9. Reflection coefficients of resistive gratings with asymmetric triangular profile.

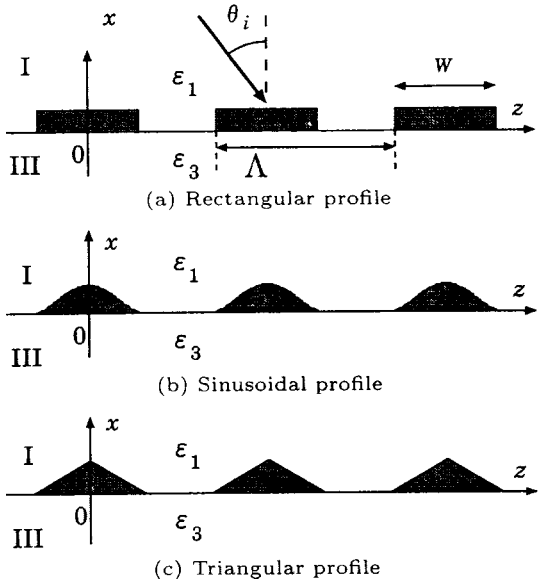

Fig. 10. Infinitely thin gratings.

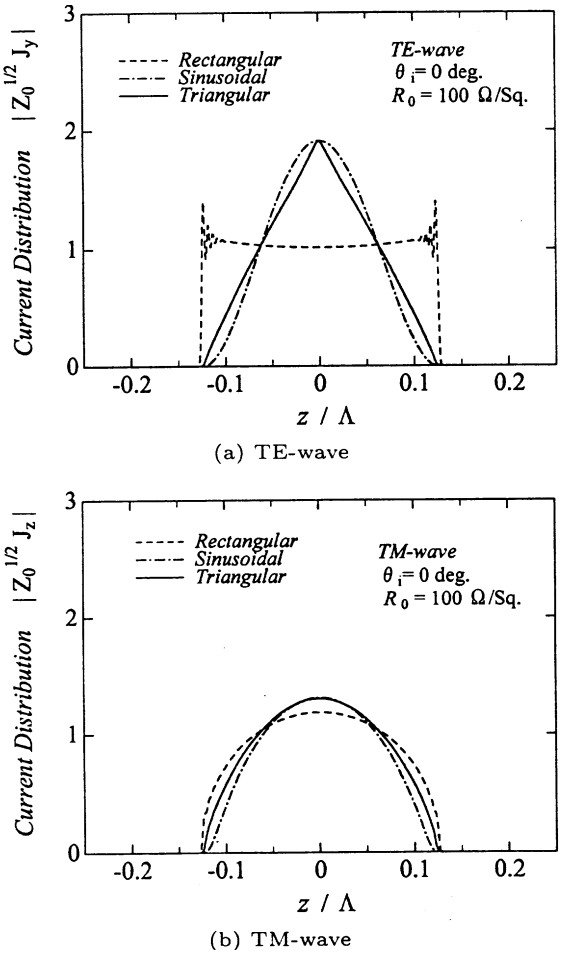

Fig. 11. Current distributions on resistive gratings.

6. Conclusions

It is shown that an infinitely thin dielectric grating with surface relief can be analyzed by using the numerical approach for a plane grating. Applying the numerical approach by solving the eigenvalue problem of the coupling matrix for a dielectric grating and the spectral Galerkin procedure for a plane grating to the same analytic model of a one-dimensional grating, some properties of the numerical calculations are investigated. In addition, some results for infinitely thin rectangular, sinusoidal, and triangular gratings obtained by the numerical approach are presented and the difference in properties between surface profiles is discussed.

REFERENCES

1. Kominami M, Wakabayashi H, Sawa S, Nakashima H. Scattering from a periodic array of arbitrary

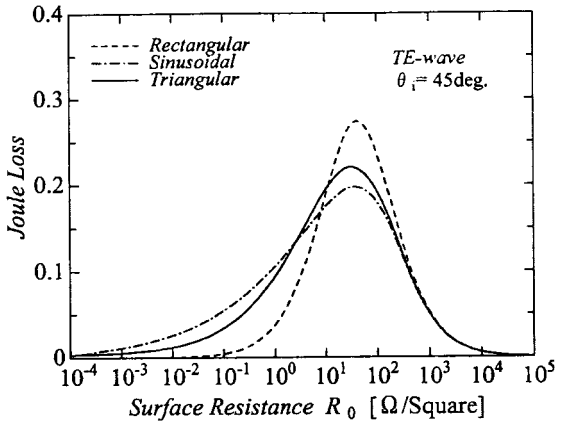

(a) TE-wave

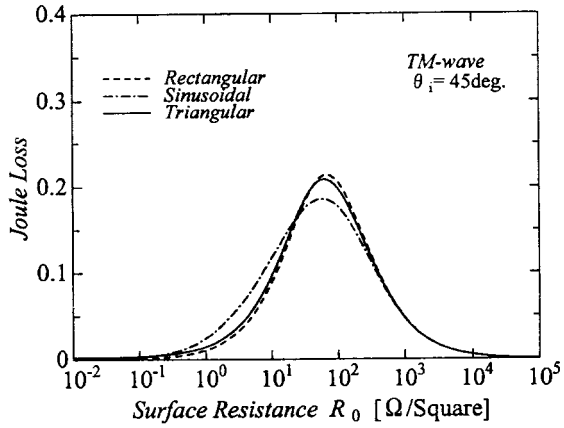

(b) TM-wave

Fig. 12. Joule losses of resistive gratings.

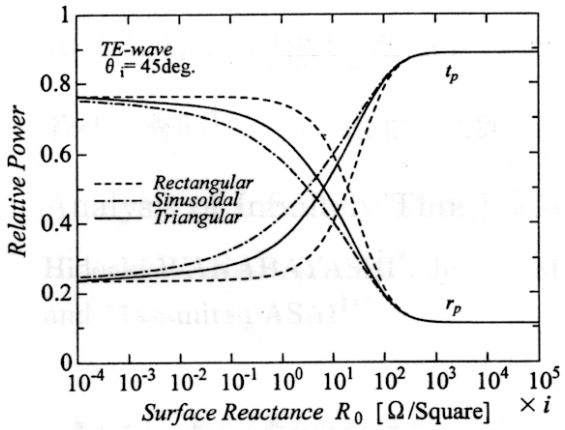

(a) TE-wave

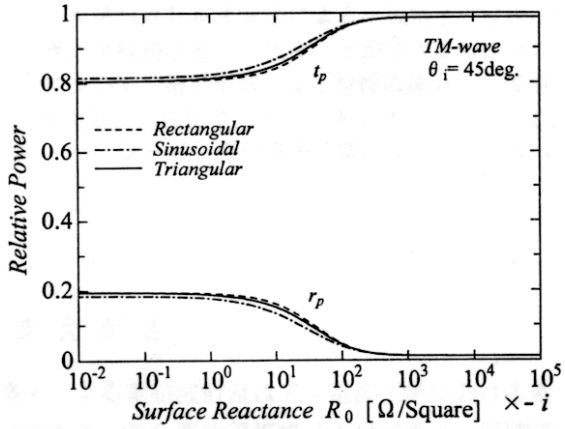

(b) TM-wave

Fig. 13. Relative power of reactive gratings.

shaped elements on a semi-infinite substrate. Trans IEICE 1993;J76-B-II:260–267.

2. Wakabayashi H, Kominami M, Kusaka H, Nakashima H. Numerical simulations for FSSs with complementary elements. IEE Microwave Antennas Propag 1994;141:477–482.
3. Asai M, Yamakita J, Sawa S, Ishii J. Analysis of two-dimensional plane gratings with anisotropic dielectric slab. IEE Japan Tech Rep EMT 1994;EMT-94-55:121–129.
4. Asai M, Yamakita J, Ishii J, Sawa S. Electromagnetic wave scattering by two-dimensional resistive plane gratings with anisotropic slab. Proc Int Conference Modeling, Simulation and Identification, IASTED, p 249–252, 1994.
5. Itoh T. In: Yamashita E, editor. Fundamental analysis of electromagnetic problems. IEICE; 1987. (in Japanese)
6. Cwik TA, Mittra R. Scattering from a periodic array of free-standing arbitrarily shaped perfectly conducting or resistive patches. IEEE Trans Antennas Propag 1987;AP-35:1226–1234.
7. Petit R, Tayeb G. Theoretical and numerical study of gratings consisting of periodic arrays of thin and lossy strips. J Opt Soc Am A 1990;7:1686–1692.
8. Wakabayashi H, Yamakita J, Asai M, Matsumoto K, Rokushima K. On the resistive boundary conditions for plane gratings. IEE Japan Tech Rep EMT 1996;EMT-96-78:45–54.
9. Wakabayashi H, Yamakita J, Matsumoto K, Asai M. Availability of approximate boundary condition for plane gratings. IEE Japan Tech Rep EMT 1997;EMT-97-9:49–54.
10. Wakabayashi H, Yamakita J, Matsumoto K, Asai M. Availability of resistive boundary conditions for plane gratings. Trans IEICE 1997;J80-C-I:387–396.

11. Wakabayashi H, Yamakita J, Matsumoto K. Scattering by thin surface-relief dielectric gratings. IEE Japan Tech Rep EMT 1997;EMT-97-78:71–76.
12. Wakabayashi H, Yamakita J, Matsumoto K. Analysis of infinitely thin dielectric gratings. IEE Japan Tech Rep EMT 1998;EMT-98-34:61–66.
13. Zinenko TL, Okuno Y, Matsushima A. Scattering of an H-polarized plane wave from a resistive grating. IEE Japan Tech Rep EMT 1996;EMT-96-79:55–65.
14. Minami K, Yamakita J, Sawa S. Analysis of lossy dielectric gratings using pseudo-periodic Green's function. Trans IEICE 1992;J75-C-I:528–535.
15. Yamakita J, Asai M, Rokushima K. Scattering fields caused by currents on anisotropic multilayered media—Green's functions on spectral domain. Trans IEICE 1990;J73-C-I:594–596.
16. Makino S, Miyahara N, Mizutamari H, Urasaki S. Design of meander-line polarizer with three layers. Trans IEICE 1988;J71-B:1358–1364.

AUTHORS (from left to right)




Hideaki Wakabayashi received his B.E. and M.E. degrees in electrical engineering from Osaka Prefecture University in 1991 and 1993. After working at Sumitomo Electric Industries, he became a research associate on the Faculty of Computer Science and System Engineering, Okayama Prefectural University, in 1994. He has been engaged in research on scattering and waveguidance problems and planar antenna.

Jiro Yamakita received his B.E. and M.E. degrees in electrical engineering from Kyoto Institute of Technology in 1969 and 1971. After working at Mitsubishi Electric Corporation, he completed his doctoral course at Osaka Prefecture University. In 1981, he became a research associate in the Department of Electrical Engineering, becoming an associate professor in 1992. Since 1993, he has been a professor in the Department of Communication Engineering, Okayama Prefectural University. He has been engaged in research on numerical algorithm for problems of waveguidance and scattering. He holds a D.Eng. degree.

Keiji Matsumoto received his B.E., M.E., and D.Eng. degrees in electrical engineering from Osaka Prefecture University in 1988, 1990, and 1994. He became a research associate in the Department of Information Systems Engineering, Osaka Sangyo University, in 1990, and an associate professor in 1996. He has been engaged in research on waveguides and scattering of electromagnetic waves. He is a member of the Optical Society of America.

Masamitsu Asai received his B.E., M.E., and Ph.D. degrees in electrical engineering from Osaka Prefecture University in 1987, 1989, and 1992. In 1992, he became a research associate in the Department of Electronics Engineering, Kinki University, and in the Department of Electronic System and Information Engineering in 1993. Since 1997, he has been an associate professor in the same Department. He was a visiting researcher in the Department of Electrical Engineering, University of Utah. He has been engaged in research on numerical analysis of electromagnetic waves. He received the IEEJ Symposium Paper Award in 1995. He is a member of IEE(Japan), IEICE(Japan), and IEEE(USA).